Published in final edited form as:
J Pediatr Gastroenterol Nutr. 2014 May ; 58(5): 561–568. doi:10.1097/MPG.0000000000000302.

Exome Sequencing Identifies a Novel *FOXP3* Mutation in a 2-Generation Family With Inflammatory Bowel Disease

David T. Okou[*], **Kajari Mondal**[†], **William A. Faubion**[‡], **Lisa J. Kobrynski**[*], **Lee A. Denson**[§], **Jennifer G. Mulle**[†], **Dhanya Ramachandran**[†], **Yuning Xiong**[‡], **Phyllis Svingen**[‡], **Viren Patel**[†], **Promita Bose**[†], **Jon P. Waters**[*], **Sampath Prahalad**[*], **David J. Cutler**[†], **Michael E. Zwick**[†], and **Subra Kugathasan**[*]

[*]Department of Pediatrics, Emory University School of Medicine, Atlanta, GA

[†]Department of Human Genetics, Emory University School of Medicine, Atlanta, GA

[‡]Division of Gastroenterology and Hepatology, Mayo Clinic, Rochester, MN

[§]Department of Pediatrics, Cincinnati Children's Hospital Medical Center, Cincinnati, OH.

Abstract

Objectives—Inflammatory bowel disease (IBD) is heritable, but a total of 163 variants commonly implicated in IBD pathogenesis account for only 25% of the heritability. Rare, highly penetrant genetic variants may also explain mendelian forms of IBD and some of the missing heritability. To test the hypothesis that rare loss-of-function mutations can be causative, we performed whole exome sequencing (WES) on 5 members of a 2-generation family of European ancestry presenting with an early-onset and atypical form of IBD.

Methods—WES was performed for all of the 5 family members; the mother and 3 male offspring were affected, whereas the father was unaffected. Mapping, annotation, and filtering criteria were used to reduce candidate variants. For functional testing we performed forkhead box P3 (FOXP3) staining and a T-cell suppression assay.

Results—We identified a novel missense variant in exon 6 of the X-linked *FOXP3* gene. The c. 694A>C substitution in *FOXP3* results in a cysteine-toglycine change at the protein position 232 that is completely conserved among all vertebrates. This variant (heterozygous in the mother and hemizygous in all 3 affected sons) did not impair FOXP3 protein expression, but significantly reduced the ability of the host's T regulatory cells to suppress an inappropriate autoimmune response. The variant results in a milder immune dysregulation, polyendocrinopathy, enteropathy, and X-linked phenotype with early-onset IBD.

Conclusions—Our study illustrates the successful application of WES for making a definitive molecular diagnosis in a case of multiply affected families, with atypical IBD-like phenotype. Our

Address correspondence and reprint requests to Subra Kugathasan, MD, Emory University School of Medicine, Division of Pediatric Gastroenterology, Emory Children's Center, 1760 Haygood Drive, Room W427, Atlanta, GA 30322 (skugath@emory.edu)..

The authors report no conflicts of interest.

results also have important implications for disease biology and disease-directed therapeutic development.

Keywords

atypical; enteropathy; exome; immune dysregulation; inflammatory bowel disease; polyendocrinopathy; X-linked

Inflammatory bowel diseases (IBDs), comprising ulcerative colitis (UC) and Crohn disease (CD), are heritable disorders of intestinal inflammation that usually manifest in the second or third decade of life. Extremely early-onset IBDs, presenting in infancy and young children, have unique characteristics and include primary immunodeficiencies that may be difficult to distinguish from chronic IBD. Recent genome-wide association studies identified >163 genetic loci for IBD (1,2), with low effect sizes that explain only 25% of the heritability in these diseases. These loci fail to explain highly penetrant, extremely early-onset IBD and some of its mendelian forms. An alternative hypothesis suggests that rare, highly penetrant genetic variants may play a major role in some forms of IBD. Recent targeted sequencing discovered rare interleukin (IL)-10/IL-10R loss-of-function variants and serves as proof-of-principle that extremely early-onset IBD cohorts are fertile targets for further gene discovery efforts (3). Whole exome sequencing (WES) has proved useful in helping clinicians make the proper diagnosis and has successfully demonstrated discordance between clinical diagnosis and molecular findings (4,5).

We ascertained a 2-generation family of 5 members, 4 of whom (the mother and her 3 sons) are affected with atypical IBD phenotypes. The youngest male member of the family (the proband) was referred to our IBD clinic and presented with atypical clinical features and phenotypes of IBD that were more diverse and severe than his siblings or his mother. For 10 years, he was given an equivocal diagnosis despite intensive and expensive investigation. In this study, we performed WES to determine whether a definitive genetic diagnosis could be made for this atypical clinical presentation.

METHODS

Patients and Clinical Evaluation

We recruited a 5-member family with the mother and 3 sons affected and the father unaffected (Fig. 1). Parents are of European ancestry and unrelated. All of the participants provided written consent, and the institutional review boards of Children's Hospital and Emory University approved all of the studies. Patient II.1 is the oldest, experiencing diarrhea in infancy, and has eczema and hypogammaglobulinemia with chronic lung disease and cutaneous candidiasis. He presented with sinusitis, food allergy, and allergic rhinitis, whereas his immunoglobulin (Ig) E and T/B cells were normal. Patient II.2, the second child, developed eczematous dermatitis, chronic candidiasis, recurrent otitis media, and pneumonia in infancy. He developed type 1 diabetes mellitus at age 3. He also developed arthritis and had intermittent diarrhea, attributed to food allergies. At age 13, he had poor specific antibody responses and did not produce IgG to φX174, despite normal total IgG levels. Serum IgE was normal. His symptoms of arthritis and recurrent infections improved

on monthly γ-globulin therapy. Patient II.3 (the proband) is the youngest; he was a full-term baby delivered after an uneventful pregnancy. He developed severe eczematous dermatitis (Fig. 2) in infancy, with recurrent bacterial skin infections. He experienced intermittent diarrhea and poor weight gain, attributed to food allergy. He had bacterial sepsis at age 2 and recurrent candidiasis, onychomycosis, and recurrent pneumonia. He developed bilateral deep venous thrombosis (DVT) at age 2 and had a recurrence of a right DVT extending into the inferior vena cava at age 5. He has unilateral right hearing loss and has not developed any endocrinopathies or autoimmune disease. His mitogen response was normal, as were his serum IgG, IgM, and IgA. Serum IgE was elevated. Colonoscopy showed evidence of multiple deep mucosal ulcerations in his colon (Fig. 3). All of the affected male members of the family shared similar phenotypes of diarrhea from food allergy and eczematous dermatitis. The patients' mother, patient I.2, has psoriasis and had a subtotal colectomy for UC. Her brother also had psoriasis and CD, and required a bone marrow transplant for aplastic anemia. The father, patient I.1, carries a diagnosis of multiple sclerosis. He has minimal symptoms, no physical limitation, and is not receiving any therapy.

Genomic DNA Isolation

Genomic DNA was extracted from patients' whole blood with a Puregene Blood Kit (Qiagen, Valencia, CA). The quantity and quality of the DNAwere determined on the NanoDrop ND-1000 spectrophotometer (Thermo Scientific, Waltham, MA), and the integrity was assessed on 1% agarose gel stained with ethidium bromide.

Array-Based Genotyping and Copy Number Variant Detection

Genotyping and copy number variant (CNV) detection were performed in all of the patients using the Genome-Wide Human SNP Array 6.0 kit (Affymetrix, Santa Clara, CA). Two aliquots of 250 ng DNA were digested with *Sty*I and *Nsp*I (New England Biolabs, Ipswich, MA), ligated with respective oligonucleotide adaptors (Affymetrix), and amplified by polymerase chain reaction (PCR) (Clontech Laboratories, Mountain View, CA). Forty-five microliters of the Agencourt AMPure-purified (Beckman Coulter, Brea, CA) DNA was fragmented and labeled (Affymetrix). The labeled DNAwas hybridized to the single nucleotide polymorphism (SNP) arrays for 16 hours, then washed, stained (Fluidics Station 450, Affymetrix), and scanned (Scanner, Affymetrix). Positive and negative controls were included for quality control. Arrays with <88% call rate, <0.4 contrast QC, or mismatched sex concordance were excluded from the analysis. Genotyping was performed using the Birdseed (version 2; Affymetrix) algorithm, as implemented in the Affymetrix Power Tool software (version 1.12.0), and used to calculate the pairwise identity by descent (*PLINKv1.07* (6)). For CNV analysis, log(2) ratio calculation was performed using the Affymetrix Power Tool. To make the CNV calls and minimize false-positives, we used 3 algorithms: GLAD (7), GADA (8), and BEAST (G.A. Satten, unpublished data). We required each CNV to have a BEAST cutoff score of 5.0 and the corresponding call to be made by at least 2 of the 3 algorithms for further analysis.

Exome Capture Library Preparation and Quality Control

Three micrograms of genomic DNA was fragmented by sonication (Covaris Inc, Woburn, MA) to yield 300-bp fragments. The fragmented DNA was purified using Agencourt's AMPure XP (Beckman Coulter), followed by polishing of the DNA ends using T4 DNA polymerase and Klenow fragment (New England Biolabs). A single “A” base overhang was added to the 3’ end of the polished DNA fragments (using Klenow fragment), followed by ligation of Illumina (San Diego, CA) paired-end adaptors with T4 DNA ligase. The ligated samples were purified using SPRI beads and amplified by 6 cycles of PCR. After size assessment (Agilent Bioanalyzer, Agilent Technologies, Santa Clara, CA) and quantitation (PicoGreen, Invitrogen, Carlsbad, CA), 1 μg of the purified library was denatured and hybridized onto the Human Exome Library version 2.0 (Roche NimbleGen, Madison, WI) by incubation at 47°C for 68 hours. Streptavidin-coated magnetic beads were used to purify the hybridized library. The hybridized library was washed, amplified during an 8-cycle PCR reaction, and then repurified for size assessment. Final quantitation of the library was performed (Kapa Biosystems Real-Time PCR assay, Wilmington, MA), and the appropriate amount was loaded onto the Illumina HiSeq2000 for paired-end (PE) sequencing.

WES

Sequencing was performed using standard Illumina protocols as described in Bentley et al (9). The exome capture libraries were diluted to 10 nmol/L and used to generate a PE cluster density of 800,000 to 900,000/mm^2. Fifty-base-pair PE sequencing was performed on the Illumina HiSeq2000 sequencer (v3 reagents).

Sequencing Data Analysis

The raw sequence reads were mapped relative to a ~30.8-Mb human exome reference sequence (NCBI37/hg19) using the PEMapper software tool (Emory University, Atlanta, GA) to identify single nucleotide variants and insertions and deletions (indels). A custom Perl script (blat_snp.pl) was used to identify the subset of variants that mapped to unique genomic regions. These unique variants were functionally annotated using SeqAnt (10), which reports the variant's type, functional classification (nonsense, replacement, silent, 5’ or 3’ untranslated region, intronic, inter-genic), presence in databases such as dbSNP, and measures of its evolutionary conservation (PhyloP, PhastCons). Data on the sequence reads, quality, and mapping have been deposited in the National Center for Biotechnology Information Sequence Read Archive (*http://www.ncbi.nlm.nih.gov/sra*; accession number, SRA071565).

Identification and Validation of Novel Functional Candidate Variants

Common variants catalogued in the dbSNP137 database (dbSNP137 also contains data from the 1000 Genomes Project) were excluded, and novel variants shared only by the affected family members (the mother and all 3 sons) were retained. Final novel coding variants consisted of those predicted to be functionally damaging by SIFT (11) and PolyPhen-2 (12). Sanger sequencing validated novel functional variants in each affected patient. Primers used for validation (Table 1) were designed using Primer3Plus (http://www.bioinformatics.nl/cgi-bin/primer3plus/primer3plus.cgi) or EmPrime (*http://primer.genetics.emory.edu*) to generate

PCR amplicons encompassing each coding variant. The amplicons were purified using Centrifugal units (Millipore, St Charles, MO) or Wizard gel and PCR cleanup (Promega, Madison, WI). The Sanger sequencing results were analyzed using SeqMan pro (version 10.1.1; DNASTAR, Madison, WI).

Cell Isolation, Flow Cytometry, and Forkhead Box P3 (FOXP3) Staining

Human T regulatory cells (Tregs) were isolated from patients or healthy donors by Ficoll separation and magnetic bead sorting ($CD4^+CD25^+$ Tregs isolation kit, 130–091–301; Miltenyi Biotec, San Diego, CA), with the addition of human CD127 antibody microbead (130–094–945) to select $CD4^+$, CD25 bright, and CD127dim T regulatory cells. FOXP3 enrichment was determined by flow cytometry in an aliquot of the final product upon cell separation. Only cells of the highest CD25 expression ($CD25^{2+}$) were selected with a limited quantity of anti-CD25 beads, as described in Beyer et al (13). Nonregulatory $CD25^-$ cells were selected by collecting flow-through from saturating amounts of anti-CD25 Ab (20 μL of anti-CD25 beads/10^7 cells). $CD4^+CD25^{2+}$ CD127dim cells are >90% FOXP3 positive, and $CD4^+CD25^-$ cells are 2% positive for FOXP3 upon intracellular staining and flow cytometry. CD4 positivity was >98% by flow cytometry, which was performed using the FACSCalibur (BD Biosciences, San Jose, CA) and 4-color staining. Commercially available antibodies for FOXP3, CD4, and CD25 (BioLegend, San Diego, CA) were used.

T-Regulatory Cell Suppression Assays

Antigen-presenting cells, $CD4^+CD25^-$ T responder cells (Tresponders), and $CD4^+CD25^+$ Tregs were isolated from 2 healthy independent control patients, patient II.3, and his mother (patient I.2). Mixed lymphocyte reactions were performed using 5×10^3 $CD4^+CD25^-$ Tresponders and 5×10^4 irradiated (at 3300 rad) T-cell–depleted antigen-presenting cells isolated from healthy blood donors. Tregs were added to cell culture at titrations of 1:32 to 1:1. The culture medium was cRPMI supplemented with 10% human serum and 2.5 μg/mL of soluble anti-CD3 (UCHT1) and anti-CD28 (BD Biosciences). Proliferation was read (in a scintillation counter) at day 7 upon addition of 1 μCi tritiated thymidine (Perkin Elmer, Waltham, MA) for the last 18 hours of culture. The suppressive phenotype of $CD25^{2+}$ cells was confirmed through in vitro suppression assays. Using Tregs from healthy donors, suppression of Tresponder proliferation at a 1:1 ratio is typically >75%.

RESULTS

Genotyping and CNV Analysis

All DNA samples were genotyped as described in the Methods section. Allele sharing was confirmed to be 50% between parents and offspring after QC filtering. We identified 2 CNVs (Table 2) that were both maternally inherited: a duplication of ~42 kb shared by all of the affected family members but containing no known gene, and a deletion of ~224 kb overlapping the *TMPRSS11E* gene, shared by the mother (I.2) and 1 affected son (II.2). Neither of the CNVs identified is known to be pathogenic or likely to explain the phenotypes seen in this family.

WES Revealed a Novel Missense Variant in the *FOXP3* Gene

For each individual, sequencing generated 5.2 to 6.6 Gb of genomic sequence, of which ~3.9 Gb was mapped relative to the human exome reference. The mapped sequence has ~129× average depth of coverage per base (Table 3). On average, 93.8% of the targeted exome sequences had >8× coverage, a threshold set to confidently call variant sites. A total of 21,180 variants (single nucleotide variants and indels) that mapped to a single unique genomic location were discovered in the 5 exomes sequenced. Variants were annotated using SeqAnt (Table 4). To identify pathogenic mutations, we assumed that variants should be novel and affect protein structure or function. Priority was given to novel exonic replacement variants, small indels, and untranslated region variants called in splice acceptor and/or donor sites because they are likely the most pathogenic. We also required that variants be shared by all of the affected family members and variants be expected to damage protein by the prediction algorithms SIFT (11) and Poly-Phen-2 (12).

After imposing these criteria, a single missense variant in the *FOXP3* gene emerged as a possible candidate. The variant was successfully validated in all of the affected family members. The mother was heterozygous, whereas all of the male offspring were hemizygous (Fig. 4). The unaffected father carried the wild-type reference nucleotide.

The novel A-to-C missense variant (c.694A>C) is in exon 6 of *FOXP3*, is predicted to be damaging by SIFT (score of 0.01) and PolyPhen-2 (score of 3.168), and replaces a cysteine (C) with a glycine (G) at position 232 (p.C232G) of the FOXP3 protein. The cysteine 232 is completely conserved among all vertebrates (Table 5). As described above, this variant was maternally inherited in all of the affected hemizygous sons, and the inheritance scenario clearly supports an X-linked recessive pattern.

Effect of Mutation on Protein Expression: Staining of Intracellular FOXP3 Protein

To determine the functional impact of the novel *FOXP3* missense variant, we assessed the expression of the FOXP3 protein in peripheral blood mononuclear cells. The percentage of $CD4^+$, $CD25^+$ $FOXP3^+$ Tregs, and the mean fluorescence intensity of FOXP3 were determined by flow cytometry in the affected proband (patient II.3) and his mother (patient I.2). Neither the absolute number nor the percent enrichment of $FOXP3^+$ cells within the $CD4^+CD25^+$ cell subset was significantly different in the proband (90.8% $FOXP3^+$, green, Fig. 5A) compared with the mother (84.5%, brown, Fig. 5A) or a healthy control (78.8%, blue, Fig. 5A). Thus, the normal expression of FOXP3 in the affected proband and his mother suggests that the c.694A>C mutation does not impair transcription and translation.

Cell Isolation and Suppressive Function of Tregs

The FOXP3 protein is considered critical for the function of $CD4^+CD25^+$ Tregs. Because the c.694A>C change did not affect protein expression, we investigated the correlation between normal FOXP3 expression and its activity (suppressive function of $CD4^+CD25^+$ Tregs).

Using irradiated $CD4^-$ cells as stimulation and $CD4^+CD25^-$ as Tresponders, Tregs from an independent healthy control, patient II.3, and patient I.2 were tested for regulatory function

via in vitro suppression assay. As demonstrated in Figure 5B, Tregs isolated from patient II. 3 (proband) could not efficiently suppress proliferation of Tresponders at 1:4, 1:2, or 1:1 ratios (Tregs:Tresponders). At 1:1 ratio, Tregs from the proband suppressed Tresponder proliferation by only 34.2% (thymidine counts 8627 ± 1583 vs 13,107 ± 539.9, mean/SE), whereas both patient I.2 (mother) and the healthy control suppressed Tresponder proliferation by >70% (mother 3780 ± 442.3 vs 13,275 ± 2365; control 4005 ± 686.5 vs 13,434 ± 342.7, Fig. 5B). These data demonstrate the functional relevance of the c.694A>C mutation.

DISCUSSION

We performed a genetic investigation of a nonconsanguineous family of 5, 4 of whom (the mother and her 3 sons) presented with an atypical chronic gastroenteritis. The 3 sons were affected with similar phenotypes of diarrhea from food allergy and eczematous dermatitis. In addition, each sibling presented with distinct clinical features (see Methods section). We performed WES on all of the members of the family, and with a pedigree consistent with a pattern of X-linkage, we focused on novel variants predicted to be damaging and that were shared by all of the affected individuals. We identified 1 novel missense variant, c.694A>C in exon 6 of the *FOXP3* gene on chromosome X, which replaces a cysteine (C) with a glycine (G) at position 232 (p.C232G) of the FOXP3 protein. All of the affected males were hemizygous for the variant, and their mother was heterozygous. Thus, the *FOXP3* c.694A>C variant is putatively causative of this atypical IBD-like phenotype.

The *FOXP3* gene provides instructions for the production of the FOXP3 protein, the master transcription factor of regulatory T cells mediating both cell development and suppressive function (14). *FOXP3* was initially discovered as the gene altered in the Scurfy mouse, leading to a fatal lymphoproliferative disorder (15,16). The *FOXP3* gene was later found to cause the immune dysregulation, polyendocrinopathy, enteropathy, X-linked syndrome (IPEX) in humans. IPEX is phenotypically similar to Scurfy and is characterized by systemic autoimmunity, typically beginning in the first year of life. All of the affected males have a common clinical triad of enteropathy, dermatitis, and endocrinopathy (17–19). Most die within the first year or 2 of life from metabolic derangements or sepsis (20), although a few patients with a milder phenotype have survived into the second or third decade of life (21–23). Therefore, a later age of onset cannot rule out an IPEX diagnosis.

To date, 40 different mutations within *FOXP3* have been described and reported in the literature (17,20,24–38) (Fig. 6). It is now clear that variable manifestations of IPEX relate directly to the precise site of the *FOXP3* mutation. Indeed, even food allergy has been attributed to *FOXP3* mutation (a deletion of a 3’ splice donor site in exon1 of the FOX3 gene (24)). Our data demonstrate the c.694A>C mutation significantly abrogates the function of FOXP3, but not expression. This scenario is reminiscent of the Wiskott-Aldrich syndrome (WAS), in which mutations in the *WAS* gene do not affect protein expression, but lead to a milder phenotype of WAS, termed X-linked thrombocytopenia (39).

Studies of the functional relevance of IPEX-inducing *FOXP3* mutations have uncovered key FOXP3 domains, including the nuclear localization signal, the protein dimerization domain,

and the DNA-binding domains. The majority of mutations identified in *FOXP3* that lead to Tregs dysfunction and typical IPEX cluster in the proline-rich (protein-protein interaction domain), leucine zipper (dimerization domain), or the forkhead domain (DNA-binding domain) of the FOXP3 protein (40). The novel c.694A>C *FOXP3* mutation affects the cysteine 232, immediately upstream (3 amino acids) of the leucine zipper domain known to specifically mediate homodimerization of FOXP3 (40–42). Furthermore, the cysteine 232 has been identified as 1 of 7 core residues (heptad repeats) of the FOXP3 coiled-coil domain, removal of which disrupts the dimerization (43) required for its function as a transcriptional regulator (40–42). These data argue strongly that the c.694A>C (p.C232G) mutation plays a causal role in this atypical extremely early-onset IBD phenotype.

To the best of our knowledge, this is the first report of a family in whom a novel c.694A>C mutation in the *FOXP3* gene leads to an atypical IBD-like phenotype representing a milder form of IPEX. This novel mutation in *FOXP3* abrogates the suppressive function of T regulatory cells. Supporting the utility of WES in familial clusters of atypical IBD, this approach led to a definitive diagnosis in this case, resulting in a justifiable treatment strategy of allogeneic bone marrow transplantation, the treatment of choice for IPEX (44).

Acknowledgment

The authors thank the family for its participation in the study.

This work was supported by National Institutes of Health grants DK087694 (S.K.), AI089714 (W.A.F.), and DK078683 (L.A.D.).

REFERENCES

1. Jostins L, Ripke S, Weersma RK, et al. Host-microbe interactions have shaped the genetic architecture of inflammatory bowel disease. Nature. 2012; 491:119–24. [PubMed: 23128233]
2. Imielinski M, Baldassano RN, Griffiths A, et al. Common variants at five new loci associated with early-onset inflammatory bowel disease. Nat Genet. 2009; 41:1335–40. [PubMed: 19915574]
3. Moran CJ, Walters TD, Guo CH, et al. IL-10R polymorphisms are associated with very-early-onset ulcerative colitis. Inflamm Bowel Dis. 2012; 19:115–23. [PubMed: 22550014]
4. Choi M, Scholl UI, Ji W, et al. Genetic diagnosis by whole exome capture and massively parallel DNA sequencing. Proc Natl Acad Sci U S A. 2009; 106:19096–101. [PubMed: 19861545]
5. Worthey EA, Mayer AN, Syverson GD, et al. Making a definitive diagnosis: successful clinical application of whole exome sequencing in a child with intractable inflammatory bowel disease. Genet Med. 2011; 13:255–62. [PubMed: 21173700]
6. Purcell S, Neale B, Todd-Brown K, et al. PLINK: a tool set for whole-genome association and population-based linkage analyses. Am J Human Genet. 2007; 81:559–75. [PubMed: 17701901]
7. Hupe P, Stransky N, Thiery JP, et al. Analysis of array CGH data: from signal ratio to gain and loss of DNA regions. Bioinformatics. 2004; 20:3413–22. [PubMed: 15381628]
8. Pique-Regi R, Monso-Varona J, Ortega A, et al. Sparse representation and Bayesian detection of genome copy number alterations from microarray data. Bioinformatics. 2008; 24:309–18. [PubMed: 18203770]
9. Bentley DR, Balasubramanian S, Swerdlow HP, et al. Accurate whole human genome sequencing using reversible terminator chemistry. Nature. 2008; 456:53–9. [PubMed: 18987734]
10. Shetty AC, Athri P, Mondal K, et al. SeqAnt: a web service to rapidly identify and annotate DNA sequence variations. BMC Bioinformatics. 2010; 11:471. [PubMed: 20854673]
11. Ng PC, Henikoff S. Predicting deleterious amino acid substitutions. Genome Res. 2001; 11:863–74. [PubMed: 11337480]

12. Ramensky V, Bork P, Sunyaev S. Human non-synonymous SNPs: server and survey. Nucleic Acids Res. 2002; 30:3894–900. [PubMed: 12202775]
13. Beyer M, Kochanek M, Darabi K, et al. Reduced frequencies and suppressive function of CD4+CD25hi regulatory T cells in patients with chronic lymphocytic leukemia after therapy with fludarabine. Blood. 2005; 106:2018–25. [PubMed: 15914560]
14. Sakaguchi S, Ono M, Setoguchi R, et al. Foxp3+ CD25+ CD4+ natural regulatory T cells in dominant self-tolerance and autoimmune disease. Immunol Rev. 2006; 212:8–27. [PubMed: 16903903]
15. Clark LB, Appleby MW, Brunkow ME, et al. Cellular and molecular characterization of the scurfy mouse mutant. J Immunol. 1999; 162:2546–54. [PubMed: 10072494]
16. Brunkow ME, Jeffery EW, Hjerrild KA, et al. Disruption of a new forkhead/winged-helix protein, scurfin, results in the fatal lymphoproliferative disorder of the scurfy mouse. Nat Genet. 2001; 27:68–73. [PubMed: 11138001]
17. Chatila TA, Blaeser F, Ho N, et al. JM2, encoding a fork head-related protein, is mutated in X-linked autoimmunity-allergic disregulation syndrome. J Clin Invest. 2000; 106:R75–81. [PubMed: 11120765]
18. Bennett CL, Christie J, Ramsdell F, et al. The immune dysregulation, polyendocrinopathy, enteropathy, X-linked syndrome (IPEX) is caused by mutations of FOXP3. Nat Genet. 2001; 27:20–1. [PubMed: 11137993]
19. Torgerson TR, Ochs HD. Immune dysregulation, polyendocrinopathy, enteropathy, X-linked syndrome: a model of immune dysregulation. Curr Opin Allergy Clin Immunol. 2002; 2:481–7. [PubMed: 14752330]
20. Gambineri E, Perroni L, Passerini L, et al. Clinical and molecular profile of a new series of patients with immune dysregulation, polyendocrinopathy, enteropathy, X-linked syndrome: inconsistent correlation between forkhead box protein 3 expression and disease severity. J Allergy Clin Immunol. 2008; 122:1105.e1–12.e1. [PubMed: 18951619]
21. Powell BR, Buist NR, Stenzel P. An X-linked syndrome of diarrhea, polyendocrinopathy, and fatal infection in infancy. J Pediatr. 1982; 100:731–7. [PubMed: 7040622]
22. Gambineri E, Torgerson TR, Ochs HD. Immune dysregulation, polyendocrinopathy, enteropathy, and X-linked inheritance (IPEX), a syndrome of systemic autoimmunity caused by mutations of FOXP3, a critical regulator of T-cell homeostasis. Curr Opin Rheumatol. 2003; 15:430–5. [PubMed: 12819471]
23. Bennett CL, Brunkow ME, Ramsdell F, et al. A rare polyadenylation signal mutation of the FOXP3 gene (AAUAAA–>AAUGAA) leads to the IPEX syndrome. Immunogenetics. 2001; 53:435–9. [PubMed: 11685453]
24. Torgerson TR, Linane A, Moes N, et al. Severe food allergy as a variant of IPEX syndrome caused by a deletion in a noncoding region of the FOXP3 gene. Gastroenterology. 2007; 132:1705–17. [PubMed: 17484868]
25. Myers AK, Perroni L, Costigan C, et al. Clinical and molecular findings in IPEX syndrome. Arch Dis Child. 2006; 91:63–4. [PubMed: 16371377]
26. Bacchetta R, Passerini L, Gambineri E, et al. Defective regulatory and effector T cell functions in patients with FOXP3 mutations. J Clin Invest. 2006; 116:1713–22. [PubMed: 16741580]
27. Gavin MA, Torgerson TR, Houston E, et al. Single-cell analysis of normal and FOXP3-mutant human T cells: FOXP3 expression without regulatory T cell development. Proc Natl Acad Sci U S A. 2006; 103:6659–64. [PubMed: 16617117]
28. Kobayashi I, Shiari R, Yamada M, et al. Novel mutations of FOXP3 in two Japanese patients with immune dysregulation, polyendocrinopathy, enteropathy, X linked syndrome (IPEX). J Med Genet. 2001; 38:874–6. [PubMed: 11768393]
29. Moudgil A, Perriello P, Loechelt B, et al. Immunodysregulation, polyendocrinopathy, enteropathy, X-linked (IPEX) syndrome: an unusual cause of proteinuria in infancy. Pediatr Nephrol. 2007; 22:1799–802. [PubMed: 17629750]
30. De Benedetti F, Insalaco A, Diamanti A, et al. Mechanistic associations of a mild phenotype of immunodysregulation, polyendocrinopathy, enteropathy, x-linked syndrome. Clin Gastroenterol Hepatol. 2006; 4:653–9. [PubMed: 16630773]

31. Lee SM, Gao B, Dahl M, et al. Decreased FoxP3 gene expression in the nasal secretions from patients with allergic rhinitis. Otolaryngol Head Neck Surg. 2009; 140:197–201. [PubMed: 19201288]
32. Halabi-Tawil M, Ruemmele FM, Fraitag S, et al. Cutaneous manifestations of immune dysregulation, polyendocrinopathy, enteropathy, X-linked (IPEX) syndrome. Br J Dermatol. 2009; 160:645–51. [PubMed: 18795917]
33. Hashimura Y, Nozu K, Kanegane H, et al. Minimal change nephrotic syndrome associated with immune dysregulation, polyendocrinopathy, enteropathy, X-linked syndrome. Pediatr Nephrol. 2009; 24:1181–6. [PubMed: 19189134]
34. Harbuz R, Lespinasse J, Boulet S, et al. Identification of new FOXP3 mutations and prenatal diagnosis of IPEX syndrome. Prenat Diagn. 2010; 30:1072–8. [PubMed: 20842625]
35. Rubio-Cabezas O, Minton JA, Caswell R, et al. Clinical heterogeneity in patients with FOXP3 mutations presenting with permanent neonatal diabetes. Diabetes Care. 2009; 32:111–6. [PubMed: 18931102]
36. An YF, Xu F, Wang M, et al. Clinical and molecular characteristics of immunodysregulation, polyendocrinopathy, enteropathy, X-linked syndrome in China. Scand J Immunol. 2011; 74:304–9. [PubMed: 21595732]
37. Suzuki S, Makita Y, Mukai T, et al. Molecular basis of neonatal diabetes in Japanese patients. J Clin Endocrinol Metab. 2007; 92:3979–85. [PubMed: 17635943]
38. Wildin RS, Ramsdell F, Peake J, et al. X-linked neonatal diabetes mellitus, enteropathy and endocrinopathy syndrome is the human equivalent of mouse scurfy. Nat Genet. 2001; 27:18–20. [PubMed: 11137992]
39. Albert MH, Bittner TC, Nonoyama S, et al. X-linked thrombocytopenia (XLT) due to WAS mutations: clinical characteristics, long-term outcome, and treatment options. Blood. 2010; 115:3231–8. [PubMed: 20173115]
40. Lopes JE, Torgerson TR, Schubert LA, et al. Analysis of FOXP3 reveals multiple domains required for its function as a transcriptional repressor. J Immunol. 2006; 177:3133–42. [PubMed: 16920951]
41. Chae WJ, Henegariu O, Lee SK, et al. The mutant leucine-zipper domain impairs both dimerization and suppressive function of Foxp3 in T cells. Proc Natl Acad Sci U S A. 2006; 103:9631–6. [PubMed: 16769892]
42. Li B, Samanta A, Song X, et al. FOXP3 is a homo-oligomer and a component of a supramolecular regulatory complex disabled in the human XLAAD/IPEX autoimmune disease. Int Immunol. 2007; 19:825–35. [PubMed: 17586580]
43. Song X, Li B, Xiao Y, et al. Structural and biological features of FOXP3 dimerization relevant to regulatory T cell function. Cell Rep. 2012; 1:665–75. [PubMed: 22813742]
44. Rao A, Kamani N, Filipovich A, et al. Successful bone marrow transplantation for IPEX syndrome after reduced-intensity conditioning. Blood. 2007; 109:383–5. [PubMed: 16990602]

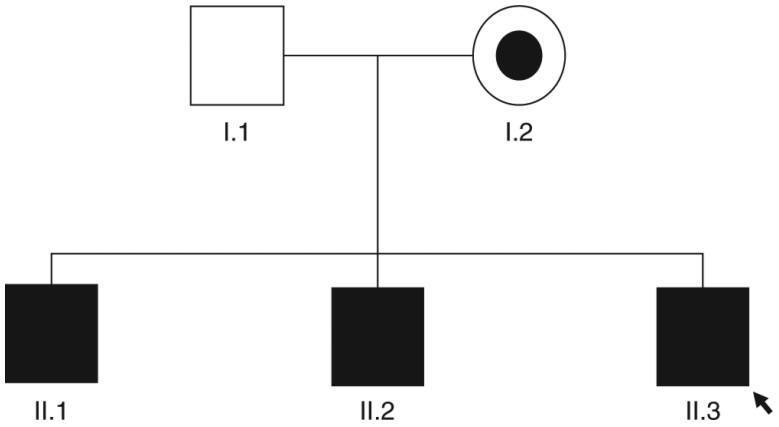

FIGURE 1.

Five individuals of European descent were recruited for exome sequencing. Square symbols are male members and the circle is the female member of the family. Filled symbols are affected individuals; partially filled symbol is the carrier individual; empty symbol is the unaffected individual; arrow indicates the proband (patient II.3).

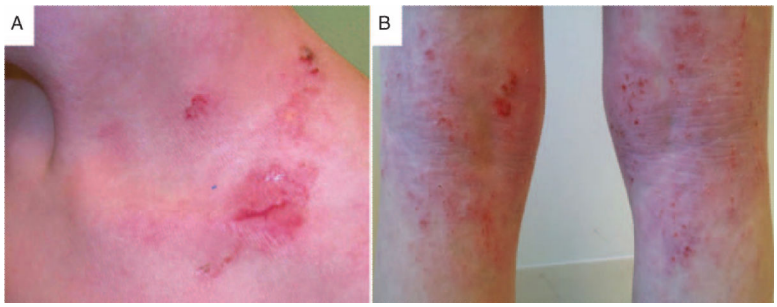

FIGURE 2.

Severe eczematous dermatitis of patient II.3 (the proband) in the supraclavicular (A) and the popliteal region (B).

FIGURE 3.

Patient II.3 colonoscopy showing multiple mucosal deep ulcerations and severe inflammation consistent with the diagnosis of inflammatory bowel disease.

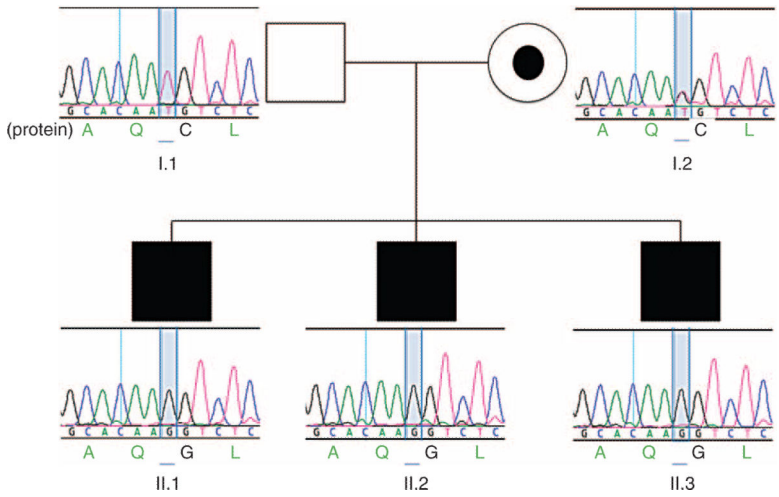

FIGURE 4.

Sequencing chromatogram of the *FOXP3* variant in each family member. DNA: A>C on (−) strand (or T>G on (+) strand). Protein: cysteine (C) to glycine (G).

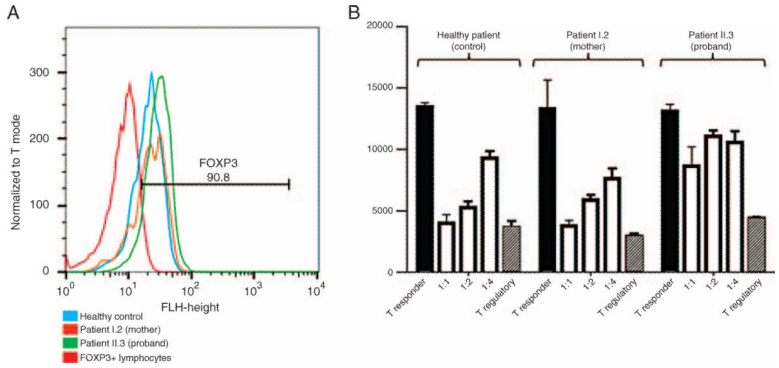

FIGURE 5.

A, Profile of flow cytometry analysis for FOXP3 (FL1 channel) staining in $CD4^{+}CD25^{+}IL7R^{lo}$ peripheral lymphocytes isolated from healthy control (blue), proband's mother (brown), and proband (green) demonstrating >90% enrichment for $FOXP3^{+}$ lymphocytes (red line, isotype control). B, $CD4^{+}CD25^{+}IL7R^{lo}$ Tregs are cocultured with increasing titer of $CD4^{+}CD25^{-}$ T responders (open histograms) from the same healthy control. Healthy control and patient I.2 demonstrate normal suppressive function with increasing titer. Patient II.3 suppresses poorly, even at a 1:1 ratio.

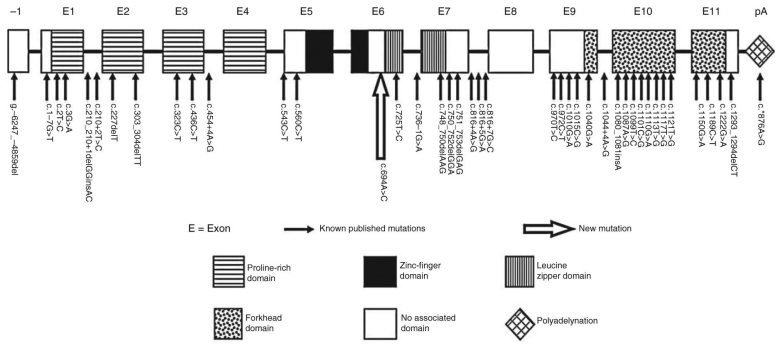

FIGURE 6.

List of all *FOXP3* gene published mutations. The novel mutation identified (represented by the big open arrow) is located between the zinc finger and the leucine zipper domain.

TABLE 1

Sequence of primers used for Sanger sequencing validation experiment (5′-3′ orientation)

Genes	Forward primer	Reverse primer
FOXP3	CTTGGTCAGTGCCATTTTCC	CTGAGGGGCATGTGTTAAGG
TUFM	GGAAACAGCCAAGTTCAACG	AGCTCTGCCTCTAGCACTGG

TABLE 2

CNVs detected in the case family

Chr:start	Size of CNV, kb	Type of CNV	Genes within the CNV	Mode of inheritance	Individual
chr1:72768904	42.23	Duplication	—	Maternal	All affected
chr4:69374929	224.60	Deletion	*TMPRSS11E*	Maternal	Patient I.2 (mother) and II.2 (2nd son)

chr = chromosome; CNV = copy number variation.

TABLE 3

Summary sequencing statistics for 5 exomes from a 2-generation family

		II.2	II.3	I.2	I.1	Average
% Reads that uniquely map to target	37.75	36.58	38.27	38.03	38.15	37.76
% Bases with at least 1 read	97.09	97.23	97.27	96.96	97.55	97.22
% Bases with at least 8× coverage	92.83	93.60	93.91	93.09	94.95	93.77
Average depth of coverage	116.65	121.37	144.62	112.38	153.22	129.65
% Exons with at least 1 read	98.30	98.41	98.41	98.30	98.31	98.35

TABLE 4

Classification of genomic variants detected from exome sequencing

		In dbSNP137		Novel	
	Total	**Count**	**% of total**	**Count**	**% of total**
Replacement SNPs	9033	8574	94.92	459	5.08
Silent SNPs	10785	10492	97.28	293	2.72
Exonic indels	72	40	55.56	32	44.44
UTR SNPs	1237	1186	95.88	51	4.12
UTR indels	9	6	66.67	3	33.33
Intronic SNPs	33	29	87.88	4	12.12
Intronic indels	3	1	33.33	2	66.67
Intergenic SNPs	8	8	100.00	0	0
Intergenic indels	0	0	0	0	0

indels = insertions and deletions; SNP = single nucleotide polymorphism; UTR = untranslated region.

TABLE 5

Comparison of *FOXP3* in vertebrates

Human	L	L	D	E	K	G	R	A	Q	**C**	L	L	Q	R	E	M	V	Q	S
Rhesus	L	L	D	E	K	G	R	A	Q	**C**	L	L	Q	R	E	M	V	Q	S
Mouse	L	L	D	E	K	G	K	A	Q	**C**	L	L	Q	R	E	V	V	Q	S
Dog	L	L	D	E	K	G	R	A	Q	**C**	L	L	Q	R	E	V	V	Q	S
Elephant	L	L	D	E	K	G	R	A	Q	**C**	L	L	Q	K	E	M	V	Q	S
Opossum	R	L	D	E	K	G	K	A	Q	**C**	L	I	Q	K	E	V	V	Q	N
Xenopus tropicalis	H	L	D	D	K	S	T	V	Q	**C**	L	L	Q	T	E	V	V	H	R
Zebrafish	A	L	D	D	K	S	T	A	Q	**C**	R	V	Q	M	E	V	V	Q	Q
Bos taurus	L	L	D	E	K	G	R	A	Q	**C**	L	L	Q	R	E	V	V	Q	S

The cysteine 232 is completely conserved among all vertebrates.